Inhibition of the Growth of Patient-Derived Pancreatic Cancer Xenografts with the MEK Inhibitor Trametinib Is Augmented by Combined Treatment with the Epidermal Growth Factor Receptor/HER2 Inhibitor Lapatinib[1,2]

Dustin M. Walters[*,3], James M. Lindberg[*,3], Sara J. Adair[*], Timothy E. Newhook[*], Catharine R. Cowan[†], Jayme B. Stokes[*], Cheryl A. Borgman[†], Edward B. Stelow[‡], Bryce T. Lowrey[*], Maria E. Chopivsky[*], Tona M. Gilmer[§], John T. Parsons[†] and Todd W. Bauer[*]

*Department of Surgery, University of Virginia Health System, Charlottesville, VA; †Department of Microbiology, Immunology and Cancer Biology, University of Virginia Health System, Charlottesville, VA; ‡Department of Pathology, University of Virginia Health System, Charlottesville, VA; §GlaxoSmithKline, Research Triangle Park, NC

Abstract

Mutations of the oncogene *KRAS* are important drivers of pancreatic cancer progression. Activation of epidermal growth factor receptor (EGFR) and human EGFR2 (HER2) is observed frequent in pancreatic adenocarcinomas. Because of co-activation of these two signaling pathways, we assessed the efficacy of inhibition of EGFR/HER2 receptors and the downstream KRAS effector, mitogen-activated protein kinase/extracellular-signal regulated kinase (ERK) kinase 1 and 2 (MEK1/2), on pancreatic cancer proliferation *in vitro* and in a murine orthotopic xenograft model. Treatment of established and patient-derived pancreatic cancer cell lines with the MEK1/2 inhibitor trametinib (GSK1120212) inhibited proliferation, and addition of the EGFR/HER2 inhibitor lapatinib enhanced the inhibition elicited by trametinib in three of eight cell lines. Importantly, in the orthotopic xenograft model, treatment with lapatinib and trametinib resulted in significantly enhanced inhibition of tumor growth relative to trametinib treatment alone in four of five patient-derived tumors tested and was, in all cases, significantly more effective in reducing the size of established tumors than treatment with lapatinib or trametinib alone. Acute treatment of established tumors with trametinib resulted in an increase in AKT2 phosphorylation that was blunted in mice treated with both trametinib and lapatinib. These data indicate that inhibition of the EGFR family receptor signaling may contribute to the effectiveness of MEK1/2 inhibition of tumor growth possibly through the inhibition of feedback activation of receptor tyrosine kinases in response to inhibition of the RAS-RAF-MEK-ERK pathway. These studies provide a rationale for assessing the co-inhibition of these pathways in the treatment of pancreatic cancer patients.

Neoplasia (2013) 15, 143–155

Introduction

Pancreatic cancer is associated with the shortest survival of any solid malignancy, and while survival has improved for most other cancers over the last several decades, the 5-year survival for pancreatic cancer remains below 5% [1]. The refractory nature of pancreatic cancers to cytotoxic and targeted therapies is likely due in part to the complex molecular signaling in pancreatic cancer [2]. The progression of pancreatic cancer from dysplasia to invasive carcinoma is accompanied by mutations in multiple genes that in turn alter core signaling and regulatory pathways [3]. Invasive cancers exhibit a high frequency of activating mutations in the KRAS oncogene, inactivation of the tumor suppressor genes p16/CDKN2A and TP53, and the inactivation of SMAD family member 4 gene (SMAD4) [4–6]. Oncogenic KRAS mutations have been reported to occur in as many as 75% to 93% of pancreatic cancers [7,8]. These observations coupled with studies showing that, in genetically engineered mice, mutation of KRAS and the deletion of TP53 or p16/CDKN2A yields pancreatic cancers with properties very similar to human pancreatic cancers [9] identify mutation of KRAS as an important driver of pancreatic cancer progression.

In addition to KRAS mutation, activation of cell surface receptor tyrosine kinases (RTKs) also plays an important role in pancreatic cancer progression. Indeed, one or more of the members of the epidermal growth factor (EGF) family of receptors is expressed in a large proportion of pancreatic cancers [10,11]. The EGF receptor (EGFR) inhibitor erlotinib is approved for use in metastatic pancreatic cancer, although its overall efficacy in clinical trials of unselected patients has been minimal [12]. A recent report shows that overexpression of HER2 receptors is an independent factor for a worse patient outcome [13]. In preclinical studies, the combination of cetuximab (anti-EGFR monoclonal antibody) and trastuzumab (anti-HER2 monoclonal antibody) exhibited a synergistic therapeutic effect on the growth of human pancreatic cancer xenografts [14]. How the activation of signaling pathways downstream of EGFR influence the constitutive signaling manifest by mutated KRAS is poorly understood but appears to play an important role in pancreatic cancer.

The mitogen-activated protein kinase (MAPK) kinase (MEK)–ERK pathway is a major therapeutic target in cancers with gain-of-function mutations in KRAS and BRAF. A number of small molecule inhibitors of both RAF and MEK1/2 are in clinical development and in early studies have proven efficacious in inhibiting the growth of RAS/RAF-driven tumors [15,16]. To provide insights into how human pancreatic cancer proliferation is impacted by therapeutic targeting of the RAS pathway, we have used a preclinical transplant model in which surgically resected human pancreatic cancers are orthotopically xenografted into immunocompromised mice. Growth and propagation of the patient-derived tumors allows the molecular, cellular, and genetic interrogation of individual tumors and assessment of their susceptibility to targeted therapy. An initial analysis of 15 patient-derived tumors shows the high frequency of expression of tyrosine-phosphorylated EGFR and less frequent expression of tyrosine-phosphorylated HER2, along with a high frequency of KRAS mutations. Because of the frequency of co-expression of oncogenic KRAS mutations and EGFR family receptors, coupled with prior evidence for the importance of both EGFR and KRAS signaling pathways, we sought to determine whether inhibition of the EGFR/HER2 receptors would augment the inhibition of pancreatic cancer proliferation caused by blocking signaling by the downstream KRAS effector, MEK1/2. Using both in vitro cell culture and mouse orthotopic xenograft models, we assessed the combined activities of lapatinib, an inhibitor of human EGFR2 (HER2) and EGFR tyrosine kinase activity [17–19], and trametinib (GSK1120212), a potent and selective allosteric inhibitor of mitogen-activated protein kinase/extracellular-signal regulated kinase (ERK) kinase 1 and 2 (MEK1/2) [20–22] with promising antitumor activity in phase I/II clinical trials [23].

We observed that while the inhibition of MEK1/2 blocked pancreatic cancer cell proliferation in all cell lines tested, we noted that the combined inhibition of EGFR/HER2 and MEK1/2 signaling augmented inhibition of cell proliferation in some but not all cell lines. Importantly, when assessed in the orthotopic xenograft model, treatment with lapatinib and trametinib resulted in significantly enhanced inhibition of tumor growth relative to trametinib treatment alone in four of five patient-derived tumors. In addition, treatment of established tumors with lapatinib and trametinib was again significantly more effective in reducing the size of established tumors than treatment with lapatinib or trametinib alone. Acute treatment of established tumors with trametinib resulted in an increase in AKT2 phosphorylation that was blunted in mice treated with both trametinib and lapatinib. These data provide evidence that inhibition of the EGFR family receptor signaling may enhance the effectiveness of MEK1/2 inhibition of tumor growth in an orthotopic setting. Recent studies of breast cancers demonstrated that inhibition of MEK1/2 signaling leads to the feedback up-regulation of RTK signaling and the reactivation of MEK-ERK [24,25]. We suggest that the action of lapatinib in combination with trametinib may be to blunt signals from treatment-dependent activation of EGF family receptors, thus augmenting the inhibition of pancreatic cancer cell proliferation. Our results provide a rationale for further experiments to assess this therapeutic combination in the treatment of pancreatic cancer patients.

Materials and Methods

Isolation and Propagation of Patient-Derived Tumors in Immunocompromised Mice

The harvest, pathologic examination, and propagation of human pancreatic cancer specimens have been described previously [26]. Human tumor tissue was resected and, following pathologic assessment, sutured onto the pancreases of 6- to 8-week-old male NOD. SCID/NCr mice. Tumors (typically arising after 3–6 months) were harvested (termed F_1) and reimplanted into 6- to 8-week-old male athymic nude mice for serial propagation (termed F_2, F_3, etc). Pathologic review was conducted for all F_0 and F_1 tumors as well as select late passage tumors, and tumor grade and stromal content were scored.

Cell Lines, Antibodies, and Inhibitors

Four pancreatic cancer cell lines, MPanc96, L3.6pl, PANC-1, and BxPC-3, were maintained as previously described [26]. The human pancreatic cancer cell line L3.6pl was kindly provided by I. J. Fidler (The University of Texas M.D. Anderson Cancer Center, Houston, TX; August 2005) [27]. MPanc-96, PANC-1, and BxPC-3 were obtained from the American Type Culture Collection (ATCC, Rockville, MD; August 2005) and maintained in Dulbecco's modified Eagle's medium (MPanc-96, PANC-1) or RPMI (BxPC3) supplemented with 10% FBS and antibiotics. Fresh patient-derived cell lines (608, 738, 366, and 450) were obtained under Institutional Review Board (IRB) protocol as previously described [26]. All cell lines were expanded, aliquoted, and frozen upon initial receipt; cells were

thawed, propagated, and used for experiments every 6 months. MPanc-96, PANC-1, and BxPC-3 were authenticated before purchase by the ATCC with cytochrome *c* oxidase subunit 1 analysis, DNA profiling, cytogenetic analysis, flow cytometry, and immunocyto-chemistry. L3.6pl cells and the fresh patient-derived cells (608, 738, 366, and 450) were authenticated in 2010 and 2011 by the University of Virginia Biomolecular Research Facility with DNA profiling, cyto-genetic analysis, flow cytometry, and immunocytochemistry. Anti-bodies used for Western blot analysis included β-actin, phospho-ERK and ERK (Sigma, St Louis, MO), EGFR (R&D Systems, Minneapolis, MN; Cell Signaling Technology, Danvers, MA), HER2/Neu (Santa Cruz Biotechnology, Santa Cruz, CA), AKT, phospho-AKT, SRC, phospho-SRC, and RAN (Cell Signaling Technology). Erlotinib was kindly provided by OSI Pharmaceuticals (Melville, NY) and lapatinib and trametinib (GSK1120212) by GlaxoSmithKline. Immunohisto-chemistry was performed as described previously [26].

Analysis of Genetic Mutations

DNA was extracted using the PureLink Genomic DNA Kit (Invitrogen, Carlsbad, CA) or from frozen tissue samples preserved in Allprotect tissue reagent using the AllPrep Kit (Qiagen, Valencia, CA). Polymerase chain reaction (PCR) amplification was carried out using BIO-X-ACT short mix (Bioline, Taunton, MA) in a Techgene (Burlington, NJ) or Mastercycler gradient (Eppendorf, Hauppauge, NY) machine using PCR primers and programs based on published protocols. Purification of the PCR product was accomplished using QIAquick Spin Kit (Qiagen), and sequence analysis was performed by the University of Virginia Biomolecular Research Facility and analyzed using the software Vector NTI (Invitrogen).

RTK and Protein Kinase Array Analysis, Western Blot Analysis, and Immunohistochemistry

The activation status of 42 RTKs and 26 protein kinases including nine MAPKs was assessed using the Proteome Profiler Human Phospho-RTK Array Kit and Human Phospho-MAPK Array Kit (R&D Systems). Briefly, cells or mechanically disrupted tumor samples were lysed directly in NP-40 lysis buffer. Lysates were cleared by centrifugation at 13,000*g* for 10 minutes and quantified by bicinchoninic acid assay (BCA). Each array was exposed to 250 µg of total protein from cell or tumor lysates. Arrays were developed using Pierce ECL Substrate (Thermo Fisher Scientific, Inc, Waltham, MA) per manufacturer's instructions and analyzed using a Bio-Rad GS-800 calibrated densitometer (Bio-Rad, Hercules, CA) and ImageQuant TL 2005 (GE Healthcare, Piscataway, NJ) software. For Western blot analysis, 20 to 25 µg of total protein was subjected to polyacrylamide gel electrophoresis–sodium dodecyl sulfate. Gels were transferred to nitrocellulose, probed with designated antibodies, and developed with ECL substrate.

In Vitro *Proliferation Assays*

Cells (1.5×10^3 to 3×10^3) were plated onto a 96-well plate in serum containing media and allowed to attach overnight. Following 1 day of growth, cell number was determined and drug treatment was initiated as indicated and replenished 48 hours later. Cells were harvested 5 days later, and the CyQUANT cell proliferation assay (Invitrogen) was used to determine relative cell number in the wells, using fluorescence measured by a plate reader (Biotek, Winooski, VT).

In Vivo *Studies*

Tumor pieces (approximately 50 mg) were orthotopically implanted onto the pancreases of 6- to 8-week-old male athymic nude mice. Tumors were allowed to grow for 1 to 2 weeks, at which point drug treatment commenced. Mice received lapatinib (65 mg/kg, orally, twice daily), trametinib (0.3 mg/kg, orally, once daily), or a combi-nation of lapatinib and trametinib. Mice underwent necropsy as indi-cated, and tumors were weighed, measured by calipers, and examined for presence of metastatic disease.

For tumor regression studies, tumors were implanted and allowed to grow to a volume of 250 to 500 mm³ as assessed by volumetric magnetic resonance imaging (MRI). Mice were then treated as above. As indicated, the dose of trametinib was increased to 1.0 mg/kg daily. MRI was used to assess tumor volume at 7- to 10-day intervals. After 3 to 4 weeks of treatment, drug was removed and tumors were allowed to grow for a period of 1 to 3 weeks.

To evaluate acute treatment response, tumors were implanted and allowed to grow for 3 to 4 weeks until palpable. Mice were then treated with vehicle control, lapatinib (65 mg/kg, orally, twice daily), trame-tinib (3 mg/kg, orally, daily), or combination therapy for 24 hours before sacrifice and tumor harvest.

MRI Assessment of Tumor Growth

For MRI, mice were anesthetized and 0.5-mm axial imaging slices were generated, encompassing the entire tumor. Tumor area was measured for each individual image slice, and tumor volume was cal-culated using the following equation: $\text{Volume}_{\text{TUMOR}} = (\text{Area}_{\text{IMAGE1}} + \text{Area}_{\text{IMAGE2}} + \text{Area}_{\text{IMAGE3}}\ldots)$ as described previously [26].

Statistical Analyses

For statistical analyses, all group comparisons were unpaired. Categorical variables were compared using either Fischer exact or Pearson chi-square tests as appropriate. Analysis of variance was used to compare continuous variables. All categorical variables have been expressed as a percentage of the group of origin, and continuous vari-ables were expressed as means ± SD. All *P* values reported are two-tailed, and statistical significance was indicated by *P* values of <.05. GraphPad Prism (Version 5.0b) software (La Jolla, CA) was used for all statistical analyses.

Results

Pathologic, Genetic, and Molecular Characterization of Tumors

Using an orthotopic transplantation model, we propagated a diverse population of surgically resected human pancreatic cancers of various stages, grades, and stromal content in the pancreases of NOD.SCID/ NCr mice [28]. Pathologic assessment of 15 patient tumors revealed 67% high-grade (grade III) tumors with 60% occurring as primary adenocarcinomas of the pancreas and 40% being derived from meta-static lesions. *KRAS* mutations were observed in 67% (codon 12), 73% had mutations in *TP53*, 71% had mutations in *SMAD4*, and 43% had mutation or methylation of *p16* (data not shown). No mutations in *BRAF* or *BRCA2* were observed and only one tumor possessed mutated *PI3K* (data not shown). Table 1 summarizes the pathologic and genetic characteristics of five representative patient-derived tumors/cell lines as

Table 1. Tumors and Cell Lines.

Tumor/Cell Line	Primary or Metastatic	Grade	Stromal Content	Genetic Alterations	
				KRAS	*p53*
608 tumor	Metastatic	High	Low	mut	mut
738 tumor	Primary	High	High	wt	mut
232 tumor	Primary	High	High	mut	mut
366 tumor	Metastatic	High	Low	mut	mut
450 tumor	Primary	Low	High	mut	mut
MPanc96	Primary	Low	High	mut	mut
L3.6pl	Metastatic	High	High	mut	wt
BxPC-3	Primary	High	Unknown	wt	mut
PANC-1	Primary	High	Low	mut	mut

mut, mutation; wt, wild type.

well as four well-characterized pancreatic cancer cell lines (MPanc96, L3.6pl, BxPC-3, and PANC-1) used in the studies described herein.

The diversity of expression of RTKs in pancreatic cancer is poorly understood. To better understand the spectrum of RTKs that may be involved in driving pancreatic cancer progression, the 15 patient-derived tumors and four cell lines were interrogated using phospho-RTK arrays formatted to detect activated (tyrosine-phosphorylated) receptors. Figure 1*A* compares the relative tyrosine phosphorylation of individual RTKs within the panel of tumors and cell lines. Robust expression of phospho-EGFR was observed in all cell lines and patient-derived tumors. In contrast, expression of phospho-HER2 was observed in only a subset (47%) of patient-derived tumors. In

addition to phospho-EGFR and phospho-HER2, we observed expression of phosphorylated fibroblast growth factor receptor 1 and 3 (FGF-R1/3) in a high proportion of patient-derived tumors, whereas expression of phosphorylated macrophage-stimulating protein (MSP) and vascular endothelial growth factor receptors were expressed at lower levels and in a small subset of patient-derived tumors.

A parallel analysis of total EGF and HER2 receptor expression was carried out in four pancreatic cell lines and cells from four patient-derived tumors using Western blot. Analysis of patient-derived tumors confirmed the expression of EGFR and HER2 in each of the tumors, although the level of expression varied substantially among the lines. HER2 expression was substantially lower than that observed in the breast cancer cell line, SK-BR-3, a cell line having amplified HER2 (Figure 1*B*). These data support previous observations of EGFR and HER2 expression in human pancreatic cancers and suggest that the activation (as measured by tyrosine phosphorylation) of these receptors can vary from tumor to tumor presumably reflecting the exposure to ligand within the microenvironment of the tumor.

Results of In Vitro Treatment with Lapatinib and MEK Inhibitor

On the basis of the frequent expression of activated EGF and HER2 receptors and the mutation of *KRAS* in a majority of the tumors, we examined the contributions of these signaling pathways on the growth of eight pancreatic cancer cell lines, four of which were derived from patient tumors within our tumor bank. Treatment of individual cell lines with 1 μM lapatinib revealed modest but statistically significant
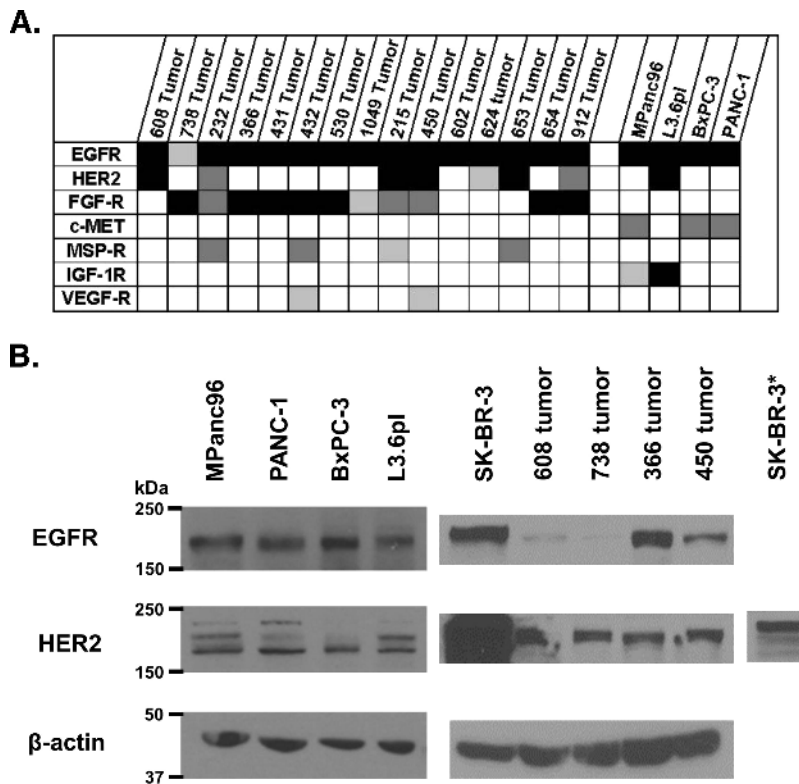

Figure 1. (A) Relative activation of selected RTKs for 15 patient-derived pancreatic cancer lysates and four established pancreatic cancer cell lines (black, more than three times the threshold; dark gray, two to three times the threshold; light gray, one to two times the threshold). (B) Western blots for EGFR and HER2 in four patient-derived pancreatic cancers, established pancreatic cancer cell lines, and SK-BR-3, a breast cancer cell line (asterisk represents a 1-s exposure).
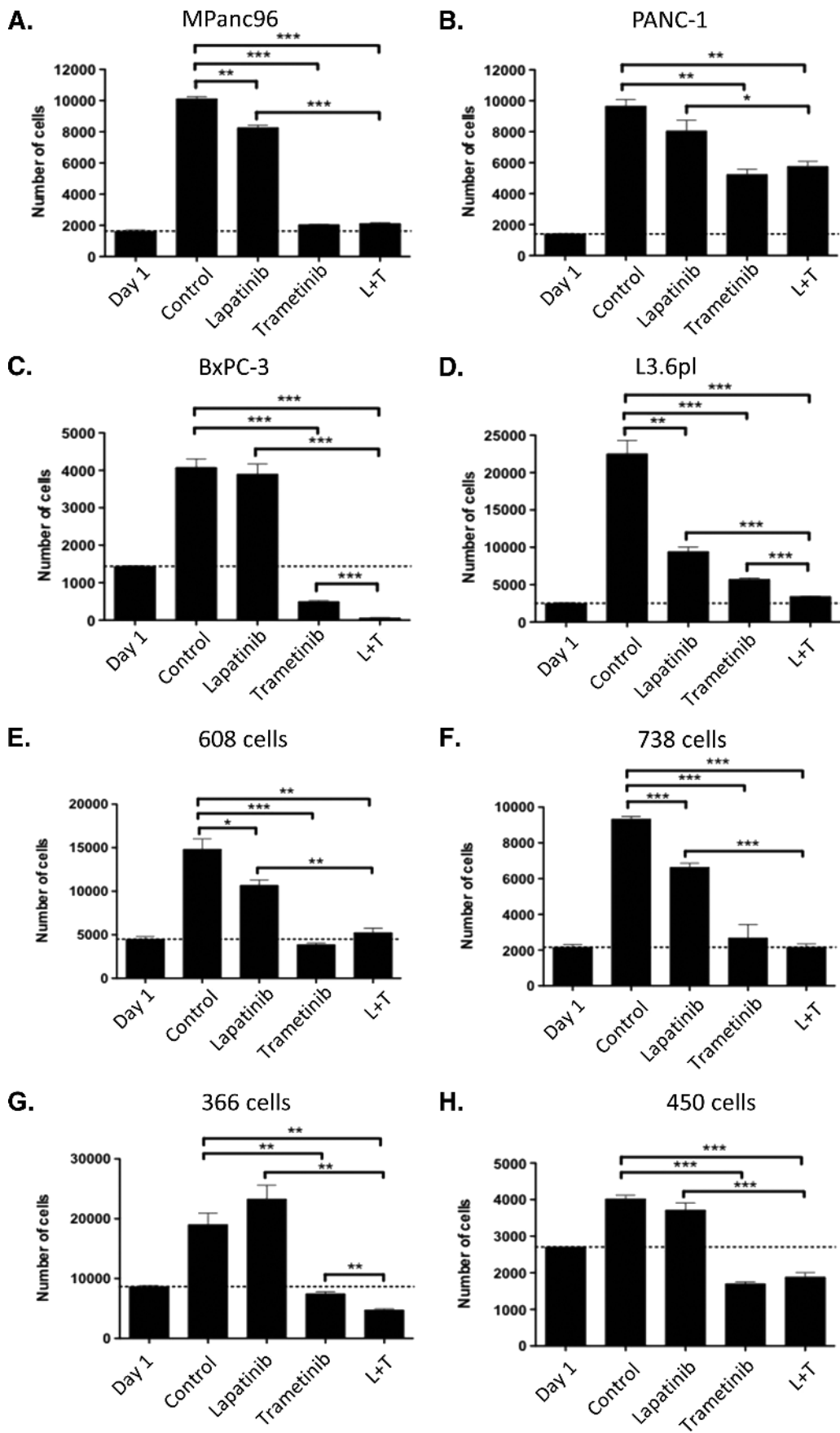
Figure 2. Proliferation assays for four established pancreatic cancer cell lines (A–D) and four patient-derived pancreatic cancer cell lines (E–H) after treatment with DMSO (control), lapatinib (1.0 μM), trametinib (0.3 μM), or combination of lapatinib and trametinib. P values are given as follows: *P < .05, **P < .01, ***P < .001.

growth inhibition in four of the eight cell lines tested in a 5-day proliferation assay (Figure 2). Treatment of the HER2-overexpressing breast cancer cell line SK-BR-3 with similar concentrations of lapatinib yielded virtually complete inhibition of growth (data not shown) consistent with the importance of this signaling pathways in these cells.

We next assessed the contribution of the MEK-ERK pathway in pancreatic cancer growth treating the individual cell lines with 0.3 µM trametinib, an allosteric inhibitor of MEK1/2 activity (Figure 2). At this concentration, inhibition of cell proliferation was observed for all cell lines, but the extent of inhibition varied from complete [i.e., below day 1 levels (indicated by the dotted lines) in BxPC-3, 366, 608, and 450 tumor cells] to 46% (PANC-1; Figure 2). Combined treatment of the panel of cell lines with both lapatinib (at 1.0 µM) and trametinib (at 0.3 µM) enhanced the inhibition of cell growth in three of the cell lines (L3.6pl, BxPC-3, and 366 cells; Figure 2). To further examine the combinatorial effects of the two inhibitors, we treated cells with 1.0 µM lapatinib and increasing concentrations of trametinib. As shown in Figure W1, BxPC-3 and 366 cells exhibited a left shift in the half-maximal inhibitory concentration (IC_{50}) when lapatinib was added to trametinib. However, most tumor-derived cell lines exhibited little alteration in the IC_{50} for proliferation when treated with both lapatinib and trametinib (data not shown). Treatment with

trametinib or the combination of lapatinib and trametinib was often cytotoxic, with fewer cells being observed at the end of the 5-day growth assay compared to the number of cells at day 1, the time of first addition of drug (Figures 2 and W1). Increased caspase-3 expression was noted in most cell lines exhibiting extensive cell death after combined treatment, consistent with an increased extent of apoptosis (data not shown).

To confirm targeting and inhibition of EGFR and HER2 receptor activity in the tumor cell lines, we treated cells with 1.0 µM lapatinib for 6 hours and interrogated cell extracts using phospho-RTK arrays. As shown in Figure 3, *A* to *C*, treatment of patient-derived cell lines led to a 72% to 92% inhibition of EGFR activity and a 94% to 98% inhibition of HER2 activity. Treatment with lapatinib had no effect on the activation status of FGF (Figure 3, *A–C*) or mesenchymal epithelial transition factor (c-MET) receptors (data not shown).

To confirm the inhibition of the MEK-ERK pathway following treatment with lapatinib, trametinib, or the combination, we treated cells with drug for 6 hours and probed cell extracts for phospho-ERK using Western blot analysis (Figure 3, *D* and *E*). Treatment with lapatinib showed variable inhibition of ERK phosphorylation, being most evident in MPanc96, BxPC-3, and 738 cells, the latter two lines wild type for *KRAS*. Treatment with trametinib or the combination of lapatinib and trametinib completely inhibited ERK phosphorylation.
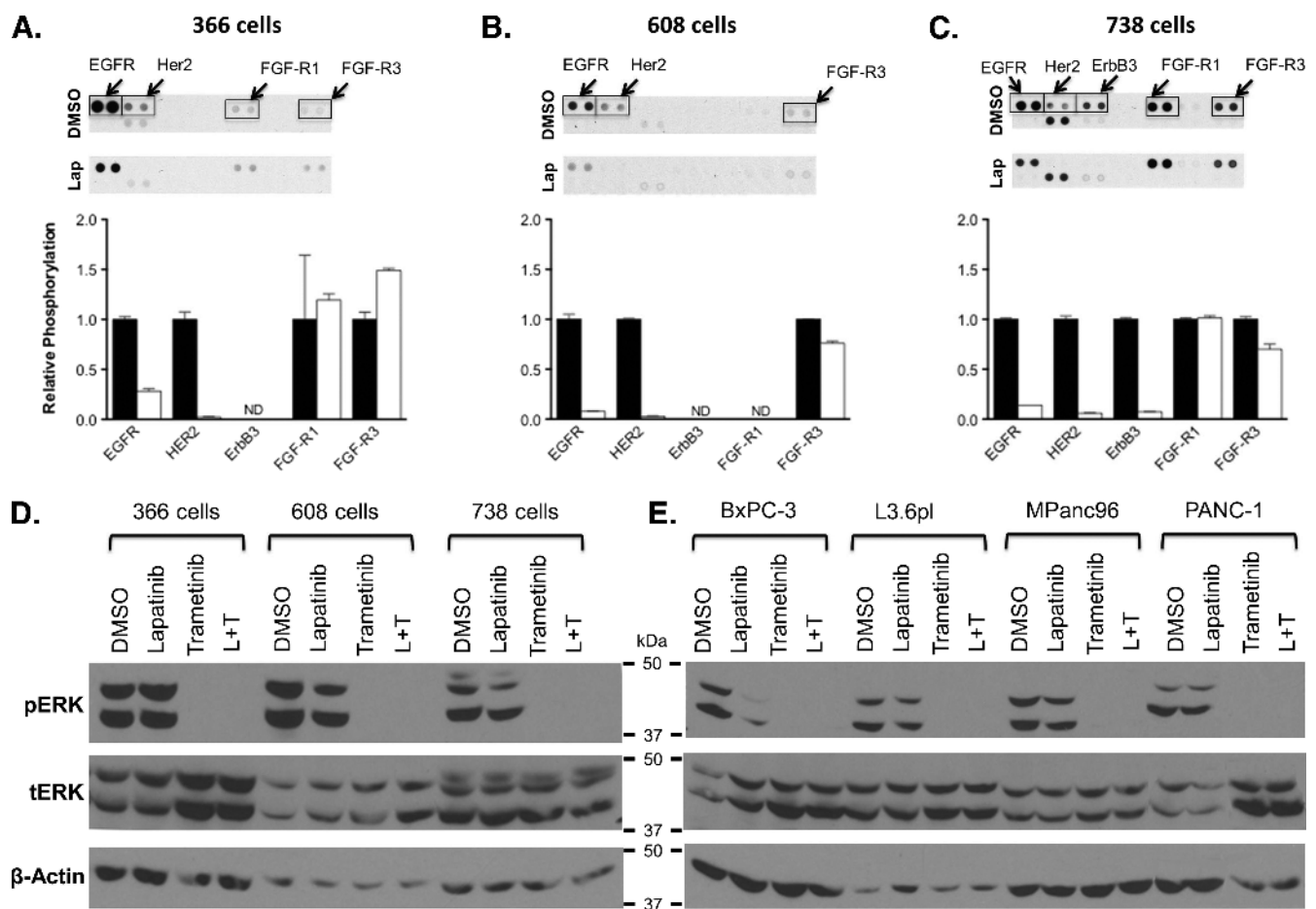

Figure 3. (A–C) Treatment of three patient-derived pancreatic cancer cell lines with DMSO (control) and lapatinib (1.0 *µ*M), showing relative phosphorylation of EGF and FGF family RTKs (ND, no detection of pRTK). (D and E) Western blot analysis for ERK and pERK in three patient-derived pancreatic cancer cell lines and four established cell lines after treatment with DMSO, lapatinib (1.0 *µ*M), trametinib (0.3 *µ*M), and combination.
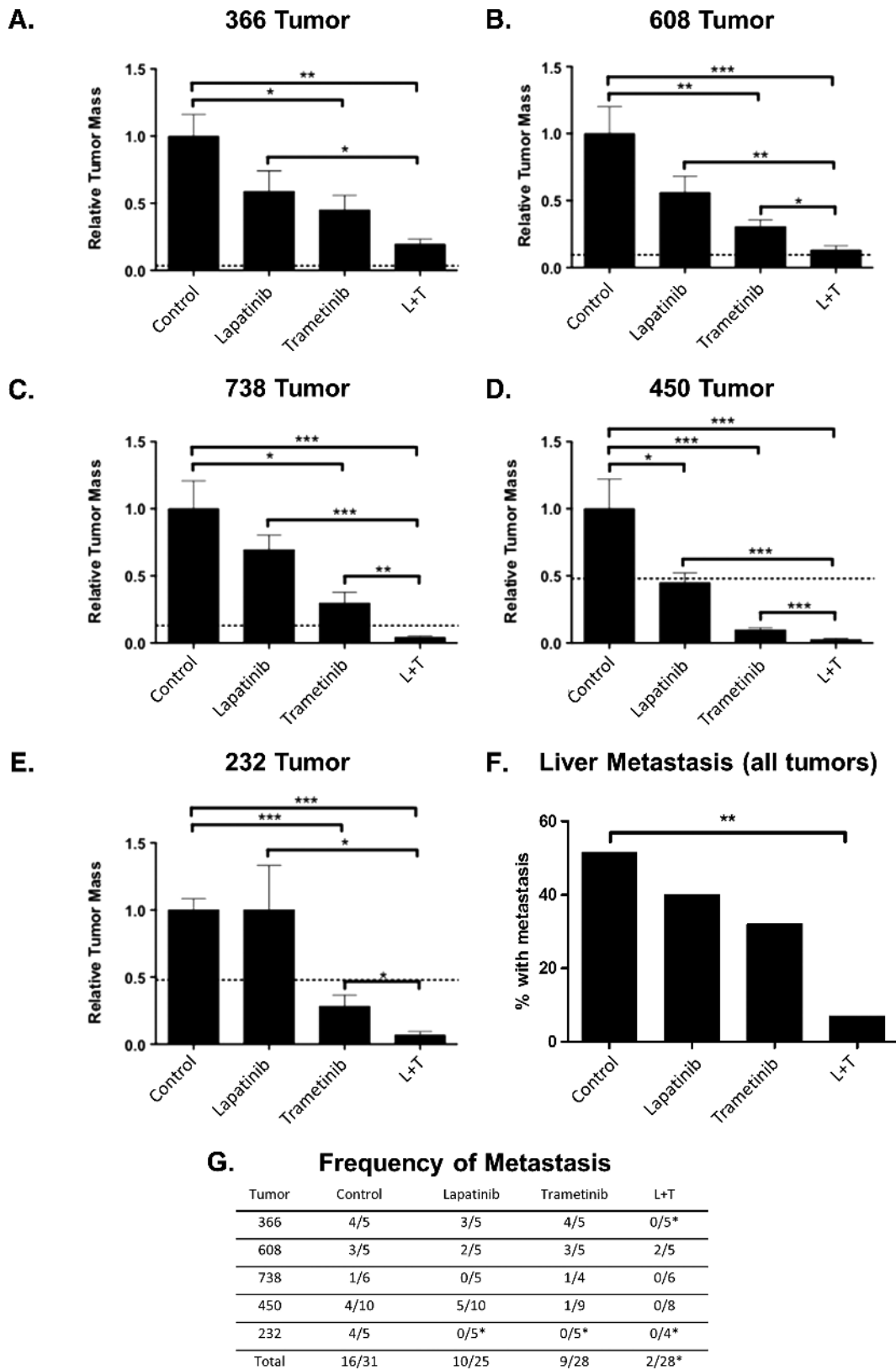
Figure 4. (A–E) *In vivo* response of five different human-derived pancreatic cancers after treatment with vehicle control, lapatinib (L; 65 mg/kg, twice daily), trametinib (0.3 mg/kg, daily), or combination (L + T). (F) Summary of liver metastasis for the same five tumors. (G) Observed liver metastases in mice bearing individual patient-derived tumors. *P* values are given as follows: *$P < .05$, **$P < .01$, ***$P < .001$.
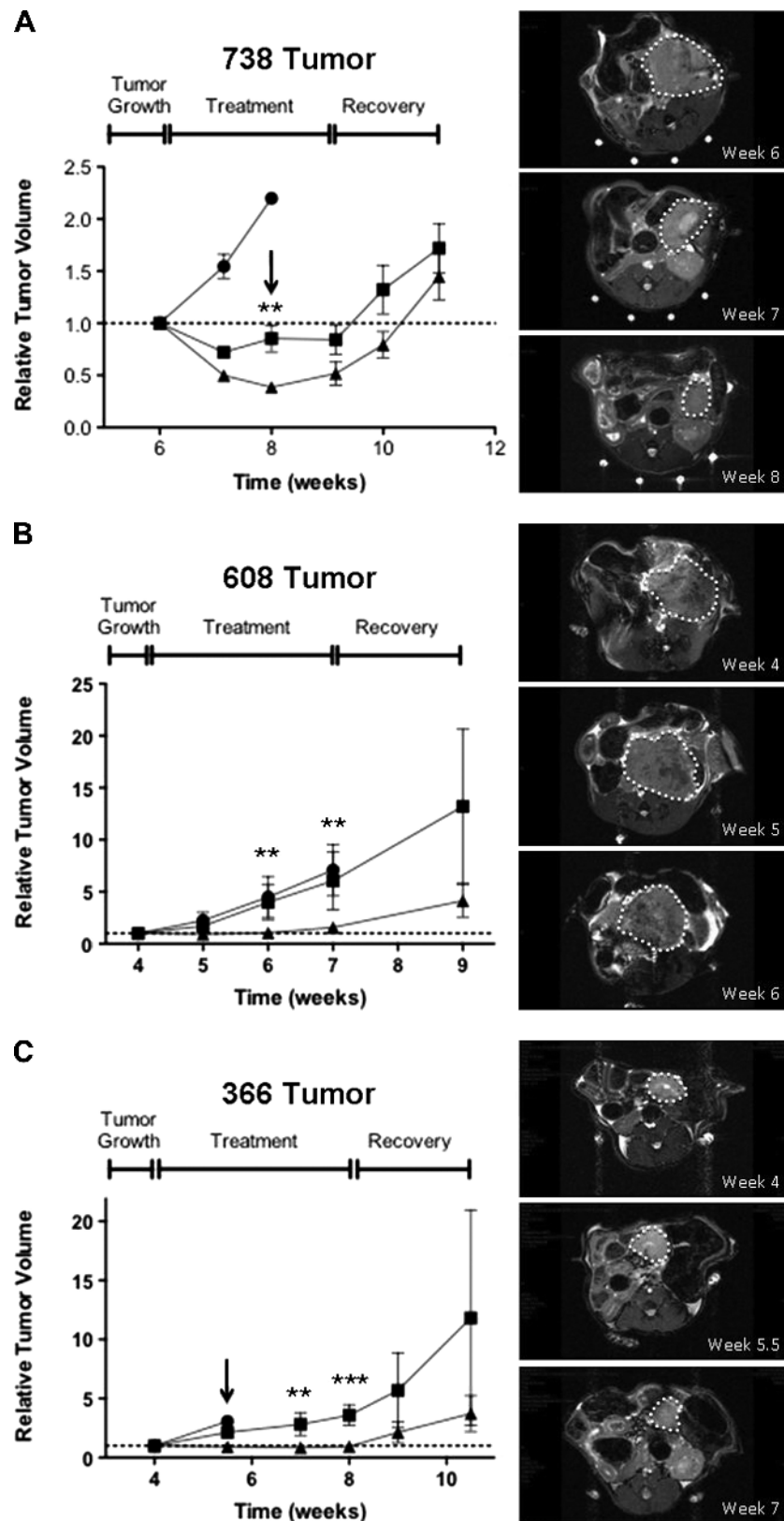
Figure 5. Response of established tumors (A–C) following treatment with lapatinib (65 mg/kg, twice daily; circles), trametinib (0.3 mg/kg, daily; squares), or combination (triangles). The tumors were allowed to grow to 250 to 500 mm^3 before the onset of treatment. Arrows denote a dose escalation of trametinib to 1.0 mg/kg daily. The right panels show MRIs at the specified time points for representative mice treated with the combination of lapatinib and trametinib with tumors outlined. P values are given as follows and indicate significance of combination treatment *versus* trametinib alone: *P < .05, **P < .01, ***P < .001.
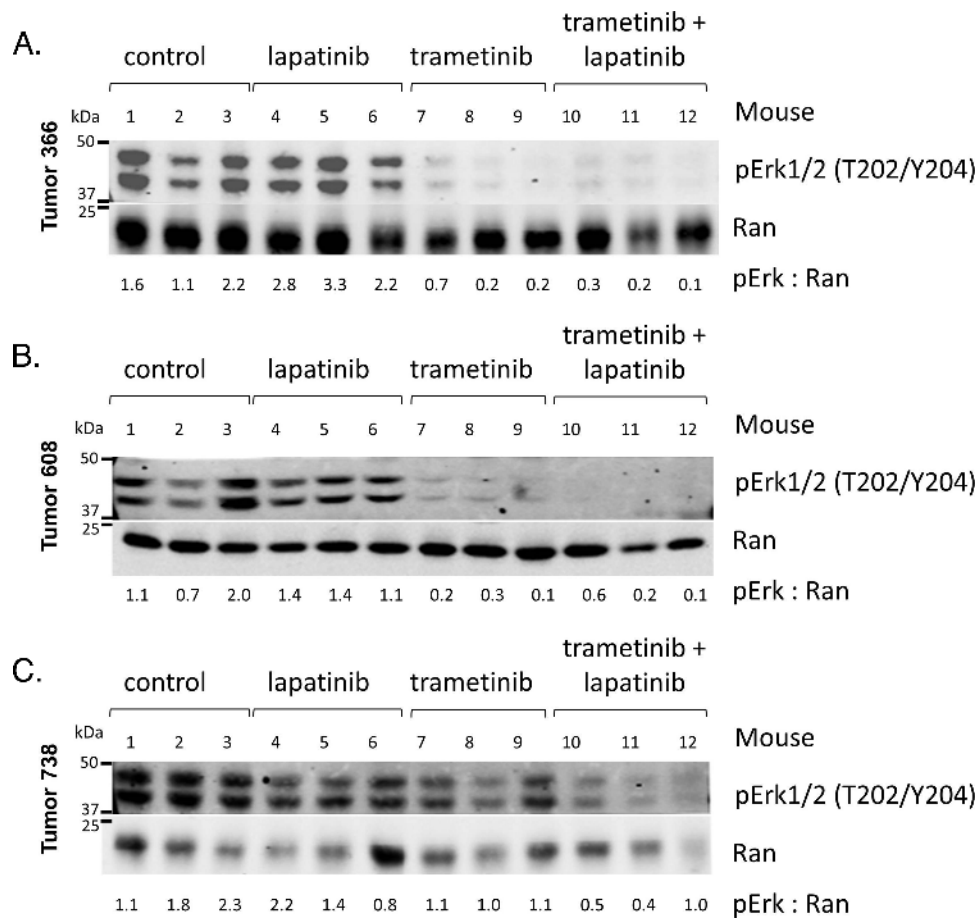
Figure 6. *In vivo* effects of inhibitor therapy on MEK1/2 signaling. Mice orthotopically implanted with patient-derived tumors 366 (A), 608 (B), and 738 (C) were treated for 24 hours with vehicle control, lapatinib (65 mg/kg, twice daily), trametinib (3 mg/kg, daily), or combination of lapatinib (65 mg/kg) and trametinib (3 mg/kg, daily) and then sacrificed. Whole tumor lysates from these animals were analyzed by Western blot analysis with the indicated antibodies. Each lane represents the tumor lysate of an individual experimental mouse exposed to the indicated treatment condition.

These data are consistent with inhibition of the MEK-ERK signaling pathway being the major determinant of the observed inhibition of cell proliferation *in vitro*. To assess the extent to which EGF-dependent pathways contribute to activation of ERK phosphorylation, we examined the response of the patient-derived 366 tumor cells to EGF stimulation in culture. As shown in Figure W2, addition of EGF to serum-starved 366 cells stimulated ERK phosphorylation approximately two-fold, showing that in spite of the mutation of *KRAS*, these tumor cells continue to respond to growth factor–mediated signals. Treatment with lapatinib blocked EGFR phosphorylation (top lanes) and dampened ERK phosphorylation. Treatment with trametinib or the combination of trametinib and lapatinib at concentrations that completely inhibited cell growth fully inhibited ERK phosphorylation as expected.

Results of In Vivo Treatment with Lapatinib and MEK Inhibitor

We next tested the efficacy of drug treatment using orthotopic implantation of patient-derived tumors into the pancreases of immuno-compromised mice. Five tumors (608, 738, 366, 232, and 450) were implanted, allowed to grow for 1 to 2 weeks, and treated with either lapatinib alone, trametinib alone, or with a combination of lapatinib

and trametinib (Figure 4). Tumors were allowed to grow for 4 to 5 weeks in the presence or absence of inhibitors, and tumor mass and presence of liver metastasis was assessed at necropsy. Only in the patient-derived 450 tumor was there a statistically significant inhibition of tumor growth upon treatment with lapatinib (65 mg/kg, twice daily; Figure 4D). Treatment with trametinib (0.3 mg/kg, daily) alone resulted in significantly better inhibition of tumor growth, with statistically significant inhibition observed in all treatment groups. Treatment with combination of lapatinib and trametinib resulted in significantly greater inhibition of tumor growth than that achieved with lapatinib in all tumors and trametinib (Figure 4, *A–E*) in four of the five tumors tested. As shown in Figure 4, *F* and *G*, treatment with a combination of lapatinib and trametinib resulted in an 84% decrease in liver metastasis compared to control-treated mice ($P < .01$) and fewer metastases than mice treated with either lapatinib or trametinib alone.

Treatment of Advanced Tumors In Vivo

To assess whether the individual treatment regimens would result in tumor stasis or regression, three different patient-derived tumors were implanted in the pancreases of immunocompromised mice and allowed to grow for 3 to 4 weeks achieving a tumor volume of 250 to 500 mm^3 as determined by MRI. Cohorts of 5 to 10 animals were

treated with lapatinib (65 mg/kg, twice daily) alone, trametinib (0.3 mg/kg, daily) alone, or a combination of lapatinib and trametinib, and tumor volume was monitored by MRI every 7 to 10 days. The 738 tumor, a *KRAS* wild-type tumor, showed no growth inhibition following treatment with lapatinib, and the animals were sacrificed after 2 weeks (Figure 5*A*). Treatment with trametinib alone resulted in a significant decrease in tumor volume after 1 week, with no significant decrease in ensuing weeks even after increasing the dosage of trametinib to 1.0 mg/kg, once daily, after 2 weeks of treatment (Figure 5*A, arrow*). Treatment with both lapatinib and trametinib resulted in significantly greater tumor regression compared to treatment with trametinib alone (60% decrease in volume after 2 weeks of treatment; Figure 5*A*). Increasing the dose of trametinib to 1.0 mg/kg, once daily, after 2 weeks in the combination group, did not enhance tumor regression. Removal of drug led to rapid tumor outgrowth in both trametinib and the combination groups within 2 weeks.

Treatment of established 608 and 366 (*KRAS* mutant) tumors yielded a different pattern of response to trametinib alone and lapa-

tinib plus trametinib therapy. The 608 and 366 tumors treated with trametinib showed a slight inhibition of growth after 1 week of treatment compared with lapatinib-treated mice, which had to be sacrificed after 1 week (366 tumor) or 3 weeks (608 tumor) of treatment due to excess tumor burden (Figure 5, *B* and *C*). In contrast, combined treatment with lapatinib and trametinib significantly inhibited further tumor proliferation and tumor size remained relatively constant over the 3- to 4-week treatment period (Figure 5, *B* and *C*). Removal of drug from the lapatinib/trametinib cohort resulted in the rapid outgrowth of the tumors within 2 to 3 weeks. In summary, the *in vivo* treatment studies clearly show that in the orthotopic setting three individual patient-derived tumors were more effectively inhibited in their growth following the combined administration of lapatinib and trametinib.

To determine the extent of MEK inhibition by trametinib *in vivo*, we treated mice bearing 250 to 500 mm^3 tumors with lapatinib, trametinib, or the combination therapy for 24 hours before sacrifice and then harvested tumors for generation of tumor lysates and analysis by Western blot and pMAPK array. As shown in Figure 6, *in vivo*
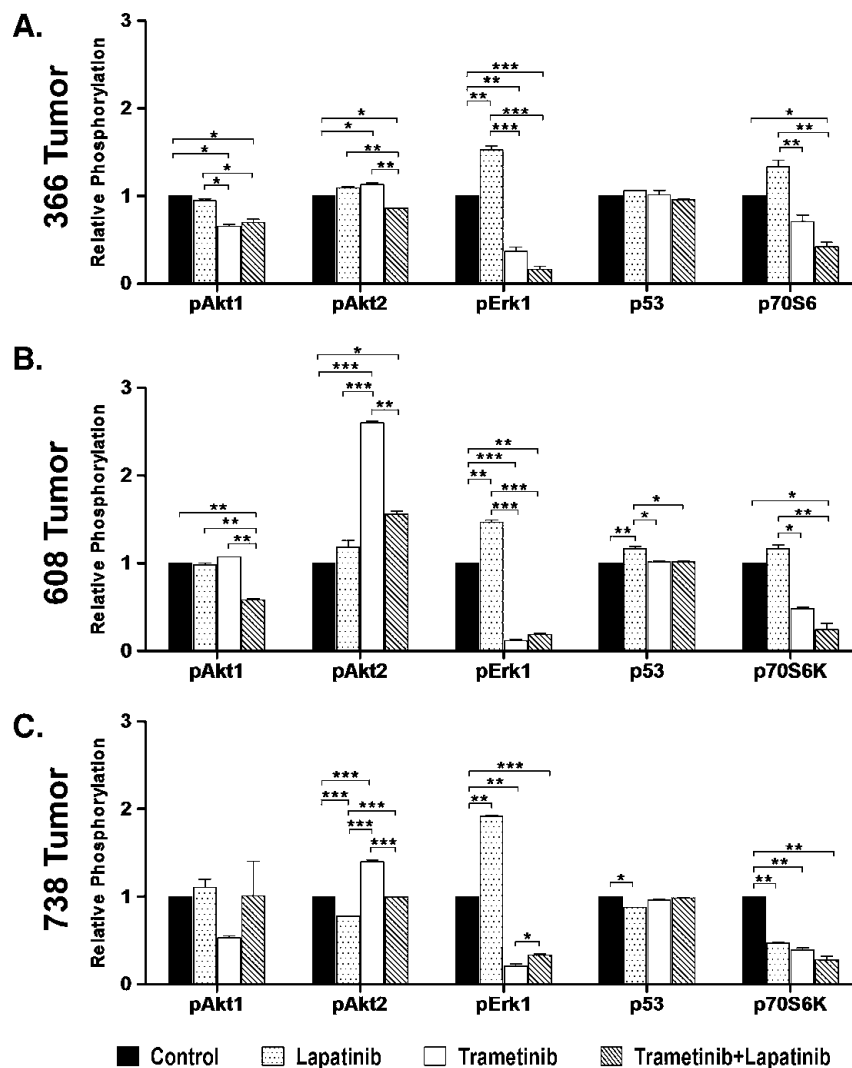

Figure 7. Relative phosphorylation of 366 tumor (*KRAS* mut), 608 tumor (*KRAS* mut), and 738 tumor (*KRAS* wt) xenografts treated with vehicle control, lapatinib (65 mg/kg, orally, twice daily), trametinib (3 mg/kg, orally, daily), or combination of trametinib and lapatinib. (A–C) Histograms depicting relative pAkt1(S473), pAkt2(S474), pErk1(T202/Y204), p53(S46), and p70S6K(T421/S424) levels in treated 366 tumor (A), 608 tumor (B), and 738 tumor (C) xenografts. Significance is denoted as ***P < .001, **P < .01, and *P < .05.

treatment with lapatinib did not substantially diminish the phosphorylation of ERK1/2. In contrast, treatment with either trametinib or the combination of trametinib and lapatinib greatly reduced ERK phosphorylation in 608 and 366 tumors (Figure 6, *A* and *B*). Interestingly, the reduction in phospho-ERK in 738 tumors was strikingly enhanced with the combination of trametinib and lapatinib (Figure 6*C*). Immunohistologic assessment of phospho-ERK paralleled the results from Western blot analysis. In all three tumors, treatment with trametinib or the combination of trametinib and lapatinib decreased the levels of phospho-ERK staining (Figure W3).

To assess how treatment impacted intracellular signaling pathways of three patient-derived tumors, we interrogated the phosphorylation of AKT isoforms (AKT1, 2, and 3), ERK 1 and 2, and p70S6 kinase using an array format. Interestingly, as shown in Figure 7, treatment of mice bearing 366, 608, or 738 tumors with trametinib yielded an increase in AKT2 phosphorylation and a significant inhibition of phosphorylation of ERK1 and p70S6 kinase (Figure 7, *A–C*; see also Figure W4). Treatment with both trametinib and lapatinib blunted the increase in AKT2 phosphorylation observed with trametinib treatment and led to a further reduction in p70S6 kinase phosphorylation. In each of the tumors, we observed a significant inhibition of pERK1 upon trametinib treatment. Phospho-p53 activity remained nearly constant between treatment groups of each assessed tumor type and is presented here a protein loading control. These results support a model in which trametinib treatment leads to increased activation of AKT2 that is blunted by combinatorial treatment with lapatinib. Both treatments have effects on the phosphorylation of ERK1 and 70S6 kinase, consistent with ERK and AKT2 being key regulators of signaling in these tumors.

Discussion

In this study, we show that concomitant inhibition of the EGFR family and MAPK pathways augments the inhibition of tumor proliferation in patient-derived pancreatic cancers propagated orthotopically in immunocompromised mice compared to treatment with either agent alone. Treatment of five patient-derived tumors, including both *KRAS* wild-type and mutant tumors, with lapatinib and trametinib resulted in enhanced inhibition of tumor growth and reduced the number of metastatic lesions compared to treatment with the single inhibitors. Importantly, treatment of larger advanced tumors with lapatinib and trametinib was significantly more effective in reducing the size of established tumors than treatment with lapatinib or trametinib alone. These observations contrast with *in vitro* results from treatment of cells cultured from patient-derived tumors or established pancreatic cancer cell lines in which treatment with lapatinib and/or trametinib resulted in the enhanced inhibition of cell proliferation in only three of eight cell lines tested. Notably, acute treatment of established tumors with trametinib resulted in an increase in AKT2 phosphorylation that was blunted in mice treated with both trametinib and lapatinib, consistent with the possibility that lapatinib in combination with trametinib may inhibit signals from treatment-dependent activation of EGF family receptors, thus augmenting the inhibition of pancreatic cancer cell proliferation. The augmented inhibitory response of patient-derived tumors to combined therapy in an orthotopic xenograft model points to the importance of the EGF signaling pathway and its contributions to tumor cell growth in the *in vivo* setting. These data underscore the importance of assessing therapeutic combinations in appropriate xenograft models.

Our studies use a representative subset of tumors taken from a panel of 15 patient-derived pancreatic tumors, two thirds of which were high-grade tumors with 60% occurring as primary adenocarcinomas of the pancreas and 40% being derived from metastatic lesions. The tumors remained both genetically and pathologically stable when propagated over several generations as orthotopic xenografts in immunocompromised mice allowing preclinical testing of drug efficacy. Oncogenic *KRAS* mutations were observed in 10 of the 15 tumors, and all mutations were in codon 12, whereas wild-type *KRAS* alleles were observed in tumors derived from both primary and metastatic lesions. A large fraction (more than 70%) of tumors exhibited mutations in *TP53* and *SMAD4*. Using phospho-RTK arrays, we observed a high frequency of activation of EGFR family RTKs, particularly EGFR (100%) and HER2 (47%). Interestingly, expression of activated FGF-R1 and 3 was observed in a high proportion of patient-derived tumors, although the significance of such activation to tumor proliferation is unclear.

Because of the prevalence of mutant *KRAS* in pancreatic cancer, signaling pathways mediated by oncogenic KRAS, particularly BRAF and MEK1/2, have been prime targets for therapeutic interdiction with small molecules [15,16,29,30]. The studies described herein use trametinib (GSK1120212) that is a potent and selective allosteric inhibitor of the MEK1 and MEK2 enzymes [20–22]. Consistent with previous studies [20,21], treatment with trametinib induced significant inhibition of proliferation (IC_{50} in the nM range), with most cell lines exhibiting either cytostatic or cytotoxic responses to treatment in a 5-day growth assay. In addition, trametinib effectively blocked activation of ERK and induced cell cycle arrest in G_1 as reported previously [31].

In orthotopically xenografted patient-derived tumors, trametinib (0.3 mg/kg) was effective in inhibiting tumor growth when administered 1 week after tumor implantation in animals. Two patient-derived tumors (450 and 232) were particularly sensitive to monotherapy with trametinib with no net tumor growth observed at necropsy after 5 weeks. In experiments, wherein tumors were allowed to grow for 4 to 5 weeks to an advanced size before treatment, trametinib treatment reduced the rate of tumor growth more effectively in the *KRAS* wild-type 738 tumor. In several experiments, increasing the dose of trametinib from 0.3 to 1 mg/kg failed to evoke greater inhibition of tumor growth, indicating that the dose of 0.3 mg/kg was sufficient for the observed biologic response. Increasing dosage of trametinib to 3 mg/kg for more that 1 week was toxic to the tumor-bearing mice (data not shown). Our studies support the conclusion that trametinib as a single agent exhibits high potency and is efficacious in inhibiting pancreatic cancer growth in culture and in an *in vivo* orthotopic xenograft model. Recent clinical studies have shown that trametinib exhibits clinical activity in melanoma and is tolerable with manageable side effects, thus paving the way for additional studies in patients with mutant *KRAS* and *BRAF* tumors [32,33].

The relative ubiquitous expression of EGFRs and the frequent expression of HER2 have made these receptors targets for therapy in pancreatic cancer [34,35]. In general, EGFR inhibitors have yielded modest effectiveness in tumor inhibition studies in mouse xenograft models [34–36]. In the experiments reported here, lapatinib treatment failed to inhibit the growth of four of the five patient-derived tumors examined. The 450 tumor, a low-grade primary adenocarcinoma, which expressed both activated EGFR and HER2, showed a statistically significant difference in growth with lapatinib treatment. Our data are consistent with the observations that only a small percentage

of pancreatic cancers will respond to lapatinib treatment alone, reflecting the relative activation of the EGFR and HER2 pathways in concert with the strong activation of signaling to MEK1/2 downstream of mutant *KRAS*.

The role of HER2 signaling in pancreatic cancers is poorly understood. In studies of patients undergoing curative resection of their pancreatic cancer, patients with HER2 overexpression had significantly shorter survival times than those with HER2 normal expression [13]. In tumor xenograft models, combined treatment with cetuximab (anti-EGFR monoclonal antibody) and trastuzumab (anti-HER2 monoclonal antibody) was shown to be superior to gemcitabine treatment in three different pancreatic cell lines [14]. Interesting, dual treatment with cetuximab and trastuzumab is reported to be associated with the disruption of EGFR/HER2 dimerization [14], suggesting that heterodimer signaling may contribute to pancreatic tumor growth. Our observations that treatment with lapatinib and trametinib provides significantly more effective inhibition of tumor growth (compared to either agent alone) in two different experimental models indicates that EGF and HER2 receptor signaling provides supportive growth signals to tumors growing in the orthotopic environment of the pancreas. Although limited to one patient-derived tumor, it is interesting that the *KRAS* wild-type tumor (738) appeared to be particularly sensitive to combined treatment, showing a more significant reduction in size following combined treatment.

The mechanism by which lapatinib augments the inhibitory effects of trametinib is unclear. One possibility is that orthotopically implanted tumors respond to factors produced by the tumor microenvironment. In support of this, we have observed that orthotopically implanted 608 tumors have readily detectable levels of amphiregulin, a well-studied ligand for EGF family receptors. Interestingly, cultured 608 cells express significantly lower levels of amphiregulin (D.M.W., J.M.L., and T.W.B., unpublished observations). Thus, *in vivo*, the proliferative response of tumors may be driven in part by ligand-dependent activation of MEK and ERK, perhaps through the normal allele of *KRAS* or perhaps through other members of the RAS family (N- or H-RAS). A second possibility is suggested by recent evidence that in breast cancer cells inhibition of MEK1/2 leads to the feedback activation/reprogramming of RTKs and increased AKT and MEK signaling [24,25]. Consistent with this possibility, we observed that *in vivo* treatment with trametinib leads to increased AKT2 phosphorylation that was blunted by lapatinib treatment. Finally, we cannot rule out that combination therapy targets signaling pathways separate to MEK and AKT that are required for tumor cell proliferation. Additional experiments will be required to explore these possible mechanisms in detail.

During the course of our studies, Diep et al. [37] reported that combination treatments of erlotinib and two MEK inhibitors, RDEA119 and AZD6244, showed significant synergistic effect compared with the corresponding single drug treatments in pancreatic cancer cell lines with wild-type *KRAS* (BxPC-3 and Hs 700T) but not in cell lines with mutant *KRAS* (MIA PaCa-2 and PANC-1). Diep et al. [37] also reported that enhanced antitumor activity was observed with combination treatment in the BxPC-3 and MIA PaCa-2 mouse subcutaneous xenograft models. Both the data presented herein and the results of Diep et al. [37] indicate that while inhibition of the MAPK pathways with trametinib or other MEK1/2 inhibitors is likely to be effective in patients with pancreatic cancer, combined therapy may provide measurable enhancement in tumor response and a rationale for consideration of this combination in clinical trials in patients with pancreatic cancer.

References

[1] Jemal A, Siegel R, Xu J, and Ward E (2010). Cancer statistics, 2010. *CA Cancer J Clin* **60**, 277–300.

[2] Hidalgo M (2010). Pancreatic cancer. *N Engl J Med* **362**, 1605–1617.

[3] Jones S, Zhang X, Parsons DW, Lin JC, Leary RJ, Angenendt P, Mankoo P, Carter H, Kamiyama H, Jimeno A, et al. (2008). Core signaling pathways in human pancreatic cancers revealed by global genomic analyses. *Science* **321**, 1801–1806.

[4] Blackford A, Serrano OK, Wolfgang CL, Parmigiani G, Jones S, Zhang X, Parsons DW, Lin JC-H, Leary RJ, Eshleman JR, et al. (2009). SMAD4 gene mutations are associated with poor prognosis in pancreatic cancer. *Clin Cancer Res* **15**, 4674–4679.

[5] Jaffee EM, Hruban RH, Canto M, and Kern SE (2002). Focus on pancreas cancer. *Cancer Cell* **2**, 25–28.

[6] Maitra A and Hruban RH (2008). Pancreatic cancer. *Annu Rev Pathol* **3**, 157–188.

[7] Shibata D, Capella G, and Perucho M (1990). Mutational activation of the c-K-ras gene in human pancreatic carcinoma. *Baillieres Clin Gastroenterol* **4**, 151–169.

[8] Smit VT, Boot AJ, Smits AM, Fleuren GJ, Cornelisse CJ, and Bos JL (1988). KRAS codon 12 mutations occur very frequently in pancreatic adenocarcinomas. *Nucleic Acids Res* **16**, 7773–7782.

[9] Hingorani SR, Wang L, Multani AS, Combs C, Deramaudt TB, Hruban RH, Rustgi AK, Chang S, and Tuveson DA (2005). Trp53R172H and KrasG12D cooperate to promote chromosomal instability and widely metastatic pancreatic ductal adenocarcinoma in mice. *Cancer Cell* **7**, 469–483.

[10] Lemoine NR (1992). The epidermal growth factor receptor in human pancreatic cancer. *J Pathol* **166**, 7–12.

[11] Kimura K, Sawada T, Komatsu M, Inoue M, Muguruma K, Nishihara T, Yamashita Y, Yamada N, Ohira M, and Hirakawa K (2006). Antitumor effect of trastuzumab for pancreatic cancer with high HER-2 expression and enhancement of effect by combined therapy with gemcitabine. *Clin Cancer Res* **12**, 4925–4932.

[12] Moore MJ, Goldstein D, Hamm J, Figer A, Hecht JR, Gallinger S, Au HJ, Murawa P, Walde D, Wolff RA, et al. (2007). Erlotinib plus gemcitabine compared with gemcitabine alone in patients with advanced pancreatic cancer: a phase III trial of the National Cancer Institute of Canada Clinical Trials Group. *J Clin Oncol* **25**, 1960–1966.

[13] Komoto M, Nakata B, Amano R, Yamada N, Yashiro M, Ohira M, Wakasa K, and Hirakawa K (2009). HER2 overexpression correlates with survival after curative resection of pancreatic cancer. *Cancer Sci* **100**, 1243–1247.

[14] Larbouret C, Gaborit N, Chardes T, Coelho M, Campigna E, Bascoul-Mollevi C, Mach JP, Azria D, Robert B, and Pelegrin A (2012). In pancreatic carcinoma, dual EGFR/HER2 targeting with cetuximab/trastuzumab is more effective than treatment with trastuzumab/erlotinib or lapatinib alone: implication of receptors' down-regulation and dimers' disruption. *Neoplasia* **14**, 121–130.

[15] Poulikakos PI and Solit DB (2011). Resistance to MEK inhibitors: should we co-target upstream? *Sci Signal* **4**, pe16.

[16] Poulikakos PI and Rosen N (2011). Mutant BRAF melanomas—dependence and resistance. *Cancer Cell* **19**, 11–15.

[17] Rusnak DW, Lackey K, Affleck K, Wood ER, Alligood KJ, Rhodes N, Keith BR, Murray DM, Knight WB, Mullin RJ, et al. (2001). The effects of the novel, reversible epidermal growth factor receptor/ErbB-2 tyrosine kinase inhibitor, GW2016, on the growth of human normal and tumor-derived cell lines *in vitro* and *in vivo*. *Mol Cancer Ther* **1**, 85–94.

[18] Wood ER, Truesdale AT, McDonald OB, Yuan D, Hassell A, Dickerson SH, Ellis B, Pennisi C, Horne E, Lackey K, et al. (2004). A unique structure for epidermal growth factor receptor bound to GW572016 (lapatinib). *Cancer Res* **64**, 6652–6659.

[19] Schwartzberg LS, Franco SX, Florance A, O'Rourke L, Maltzman J, and Johnston S (2010). Lapatinib plus letrozole as first-line therapy for HER-2+ hormone receptor–positive metastatic breast cancer. *Oncologist* **15**, 122–129.

[20] Gilmartin AG, Bleam MR, Groy A, Moss KG, Minthorn EA, Kulkarni SG, Rominger CM, Erskine S, Fisher KE, Yang J, et al. (2011). GSK1120212 (JTP-74057) is an inhibitor of MEK activity and activation with favorable pharmacokinetic properties for sustained *in vivo* pathway inhibition. *Clin Cancer Res* **17**, 989–1000.

[21] Yamaguchi T (2011). Antitumor activities of JTP-74057 (GSK1120212), a novel MEK1/2 inhibitor, on colorectal cancer cell lines *in vitro* and *in vivo*. *Int J Oncol* **39**, 23–31.

[22] Yamaguchi T, Yoshida T, Kurachi R, Kakegawa J, Hori Y, Nanayama T, Hayakawa K, Abe H, Takagi K, Matsuzaki Y, et al. (2007). Identification of JTP-70902, a p15INK4b-inductive compound, as a novel MEK1/2 inhibitor. *Cancer Sci* **98**, 1809–1816.

[23] Infante JR, Matsubayashi H, Sato N, Tonascia J, Klein AP, Riall TA, Yeo C, Iacobuzio-Donahue C, and Goggins M (2007). Peritumoral fibroblast SPARC expression and patient outcome with resectable pancreatic adenocarcinoma. *J Clin Oncol* **25**, 319–325.

[24] Duncan JS, Whittle MC, Nakamura K, Abell AN, Midland AA, Zawistowski JS, Johnson NL, Granger DA, Jordan NV, Darr DB, et al. (2012). Dynamic reprogramming of the kinome in response to targeted MEK inhibition in triple-negative breast cancer. *Cell* **149**, 307–321.

[25] Mirzoeva OK, Das D, Heiser LM, Bhattacharya S, Siwak D, Gendelman R, Bayani N, Wang NJ, Neve RM, Guan Y, et al. (2009). Basal subtype and MAPK/ERK kinase (MEK)-phosphoinositide 3-kinase feedback signaling determine susceptibility of breast cancer cells to MEK inhibition. *Cancer Res* **69**, 565–572.

[26] Stokes JB, Adair SJ, Slack-Davis JK, Walters DM, Tilghman RW, Hershey ED, Lowrey B, Thomas KS, Bouton AH, Hwang RF, et al. (2011). Inhibition of focal adhesion kinase by PF-562,271 inhibits the growth and metastasis of pancreatic cancer concomitant with altering the tumor microenvironment. *Mol Cancer Ther* **10**, 2135–2145.

[27] Bruns CJ, Harbison MT, Kuniyasu H, Eue I, and Fidler IJ (1999). *In vivo* selection and characterization of metastatic variants from human pancreatic adenocarcinoma by using orthotopic implantation in nude mice. *Neoplasia* **1**, 50–62.

[28] Walters DM, Adair SJ, Stokes JB, Borgman C, Lowrey B, Adams RB, Fox JW, Papin JA, Parsons JT, and Bauer TW (2010). *Proceedings of the 101st Annual Meeting of the American Association for Cancer Research—Proceedings Supplement: Late-Breaking Abstracts*. AACR, Washington, DC. p. 46Abstract No. LB-148.

[29] Friday BB and Adjei AA (2008). Advances in targeting the Ras/Raf/MEK/Erk mitogen-activated protein kinase cascade with MEK inhibitors for cancer therapy. *Clin Cancer Res* **14**, 342–346.

[30] Wang D, Boerner SA, Winkler JD, and LoRusso PM (2007). Clinical experience of MEK inhibitors in cancer therapy. *Biochim Biophys Acta* **1773**, 1248–1255.

[31] Gysin S, Lee SH, Dean NM, and McMahon M (2005). Pharmacologic inhibition of RAF→MEK→ERK signaling elicits pancreatic cancer cell cycle arrest through induced expression of p27^{Kip1}. *Cancer Res* **65**, 4870–4880.

[32] Infante JR, Fecher LA, Falchook GS, Nallapareddy S, Gordon MS, Becerra C, DeMarini DJ, Cox DS, Xu Y, Morris SR, et al. (2012). Safety, pharmacokinetic, pharmacodynamic, and efficacy data for the oral MEK inhibitor trametinib: a phase 1 dose-escalation trial. *Lancet Oncol* **13**, 773–781.

[33] Falchook GS, Lewis KD, Infante JR, Gordon MS, Vogelzang NJ, DeMarini DJ, Sun P, Moy C, Szabo SA, Roadcap LT, et al. (2012). Activity of the oral MEK inhibitor trametinib in patients with advanced melanoma: a phase 1 dose-escalation trial. *Lancet Oncol* **13**, 782–789.

[34] Harsha HC, Jimeno A, Molina H, Mihalas AB, Goggins MG, Hruban RH, Schulick RD, Kamath U, Maitra A, Hidalgo M, et al. (2008). Activated epidermal growth factor receptor as a novel target in pancreatic cancer therapy. *J Proteome Res* **7**, 4651–4658.

[35] Jimeno A, Tan AC, Coffa J, Rajeshkumar NV, Kulesza P, Rubio-Viqueira B, Wheelhouse J, Diosdado B, Messersmith WA, Iacobuzio-Donahue C, et al. (2008). Coordinated epidermal growth factor receptor pathway gene overexpression predicts epidermal growth factor receptor inhibitor sensitivity in pancreatic cancer. *Cancer Res* **68**, 2841–2849.

[36] Komoto M (2010). *In vitro* and *in vivo* evidence that a combination of lapatinib plus S-1 is a promising treatment for pancreatic cancer. *Cancer Sci* **101**, 468–473.

[37] Diep CH, Munoz RM, Choudhary A, Von Hoff DD, and Han H (2011). Synergistic effect between erlotinib and MEK inhibitors in KRAS wild-type human pancreatic cancer cells. *Clin Cancer Res* **17**, 2744–2756.
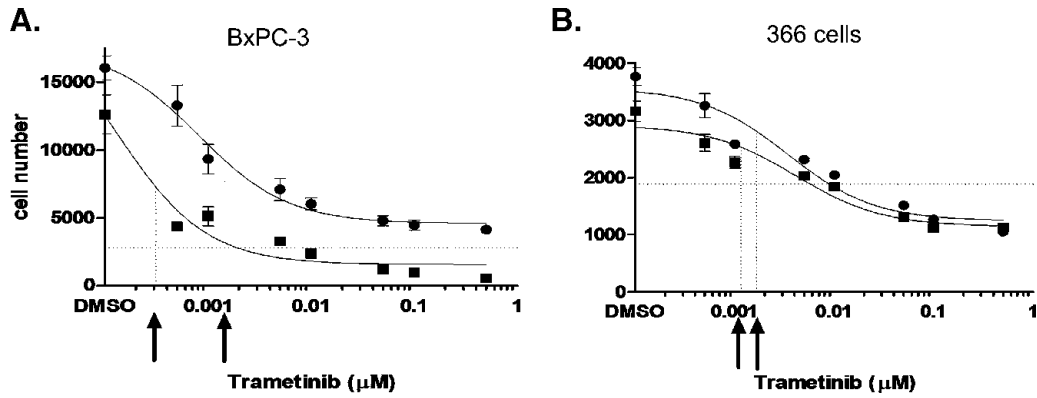
Figure W1. Dose-response curves for BxPC-3 (A), an established pancreatic cancer cell line, and 366 (B), a patient-derived cell line. Circles represent trametinib (GSK1120212) alone, and squares are trametinib (GSK1120212) in combination with 1.0 μM lapatinib. Horizontal dotted line indicates cell number initially plated. Vertical dotted lines indicate IC_{50} for each treatment.
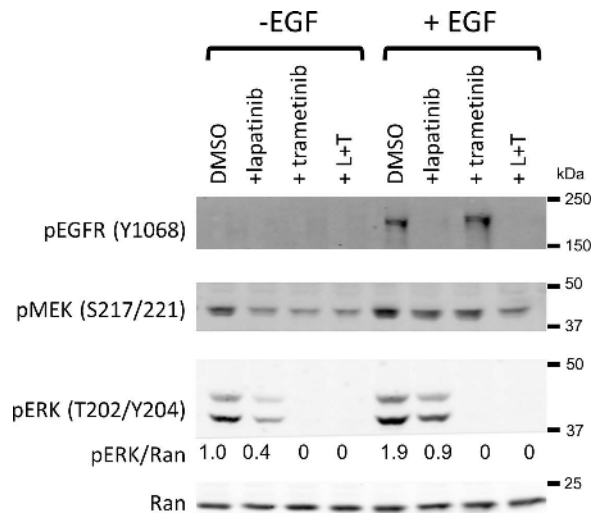

Figure W2. (A) 366 Cells were serum starved for 4 hours and then treated with either 1 μM lapatinib, 0.3 μM trametinib, or the combination (+L+T) for 1 hour before being stimulated with 100 ng/ml EGF for 30 minutes. pERK and Ran were quantitated and pERK was divided by Ran to determine changes in phosphorylation. Phosphorylated protein level was divided by total protein level to yield quantitative values.
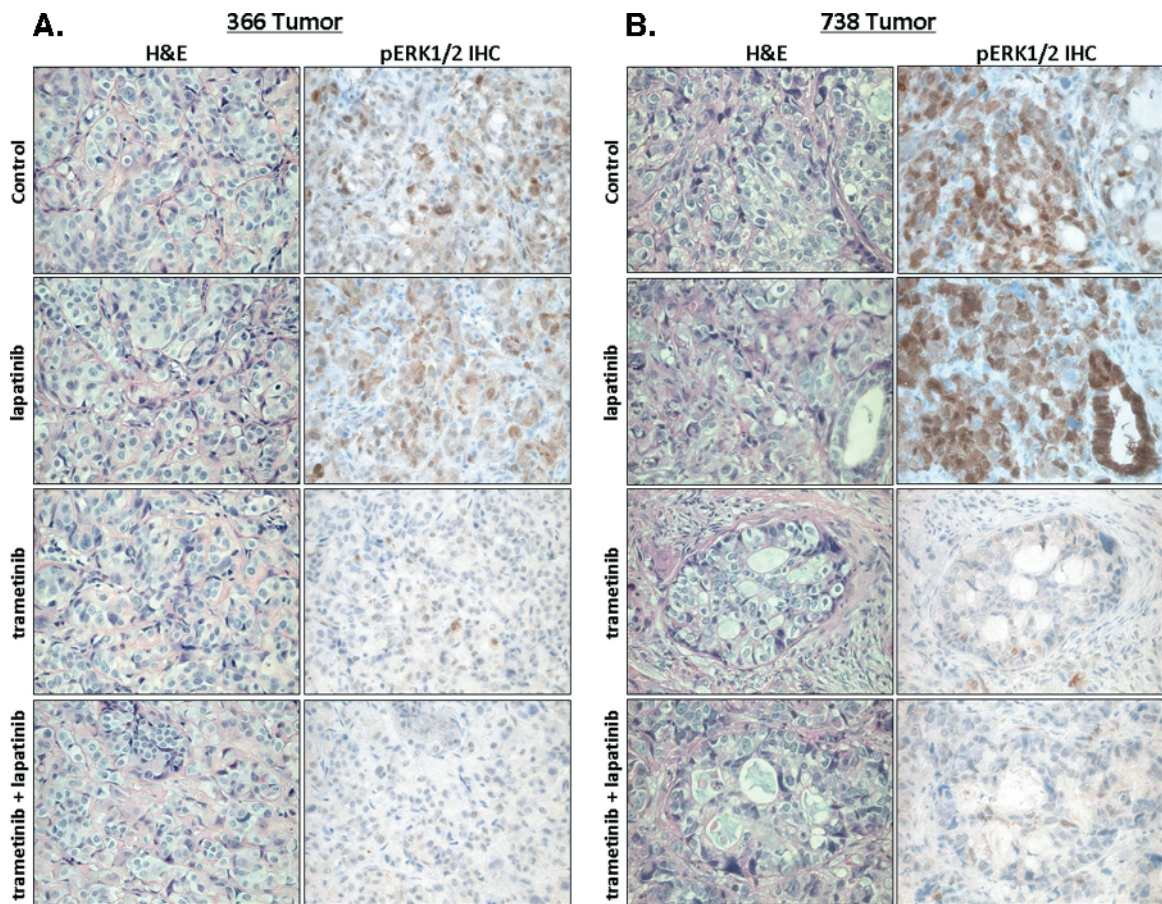
Figure W3. *In vivo* effect of lapatinib and trametinib on ERK1/2 phosphorylation measured by immunohistochemistry. Representative micrographs (original magnification, ×40) from patient-derived orthotopic tumor xenografts [(A) 366 tumor and (B) 738 tumor] treated for 24 hours with vehicle control, lapatinib (65 mg/kg, twice daily), trametinib (3 mg/kg, daily), or combination therapy. Phospho-ERK1/2 most intensely stains the pancreatic ductal adenocarcinoma cells in the control and lapatinib-treated mice, while limited or no staining is observed in trametinib- and combination-treated mice.
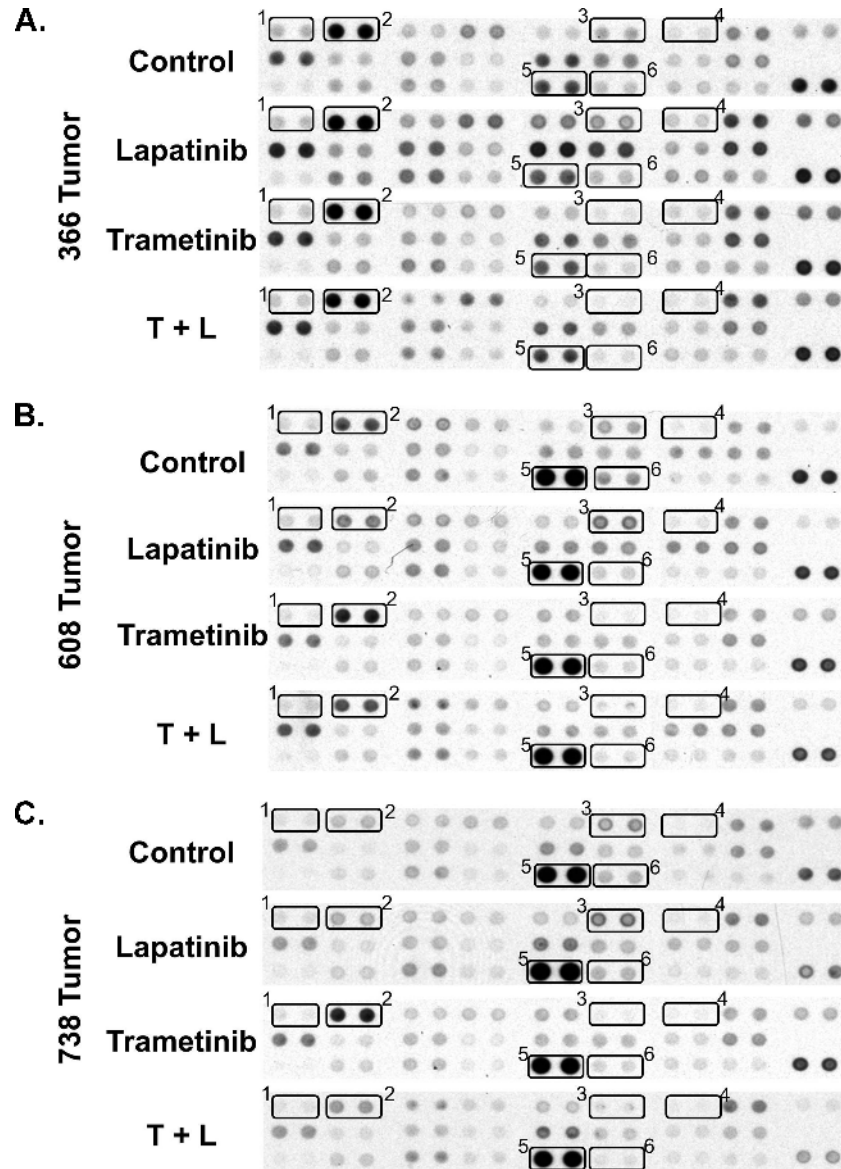
Figure W4. Relative phosphorylation of 366 tumor (*KRAS* mut), 608 tumor (*KRAS* mut), and 738 tumor (*KRAS* wt) xenografts treated with vehicle control, lapatinib (65 mg/kg, orally, twice daily), trametinib (3 mg/kg, orally, daily), or combination of trametinib and lapatinib (T + L). (A–C) Representative images of pMAPK arrays of whole tumor lysates from 366 tumor (A), 608 tumor (B), and 738 tumor (C) xenografts under the above treatment conditions. Relative pAkt1 (1), pAkt2 (2), pErk1 (3), pErk2 (4), p53 (5), and p70S6 kinase (6) levels are highlighted.